torus. The observations do not remove the possibility of a simultaneous magnetotail aurora, but if present it must not be a dominant component. The power required to drive the aurora by precipitated electrons stopped in the atmosphere is 1.7×10^{14} W, and the energy flux is comparable to that in an IBC (international brightness coefficient) III aurora on Earth (*13*). The continuous deposition of this amount of energy must have a measurable global effect on the atmosphere of Jupiter. The auroral activity may in fact be indirectly related to the discovery (reported here) of a general deposition of particle energy on the dayside hemisphere, most plausibly in electrons, of 5 erg cm^{-2} sec^{-1}. Much of this energy flux must end in atmospheric heating.

Finally, successful solar and stellar occultation observations have been obtained, and we expect the measurements to yield significant results on atmospheric structure pending extensive analysis with the aid of atmospheric models.

B. R. SANDEL
D. E. SHEMANSKY
A. L. BROADFOOT
Space Sciences Institute, University of Southern California Tucson Laboratories, Tucson, Arizona 85713
J. L. BERTAUX
J. E. BLAMONT
Service D'Aeronomie du CNRS, Paris, France
M. J. S. BELTON
Kitt Peak National Observatory, Tucson, Arizona 85726
J. M. AJELLO
Jet Propulsion Laboratory, Pasadena, California 91103
J. B. HOLBERG
Planetary Science Institute, Pasadena, California 91101
S. K. ATREYA
T. M. DONAHUE
University of Michigan, Ann Arbor 48109
H. W. MOOS
Johns Hopkins University, Baltimore, Maryland 21218
D. F. STROBEL
Naval Research Laboratory, Washington, D.C. 20375
J. C. MCCONNELL
York University, Ontario, Canada M3J 1P3
A. DALGARNO
R. GOODY
M. B. MCELROY
Harvard University, Cambridge, Massachusetts 02138
P. Z. TAKACS
Brookhaven National Laboratories, Upton, New York 11973

References and Notes

1. A. L. Broadfoot *et al.*, *Science* **204**, 979 (1979).
2. D. E. Shemansky, in preparation.
3. R. A. Brown, *Astrophys. J.* **224**, L97 (1978).
4. J. T. Trauger, G. Münch, F. L. Roesler, paper presented at the American Geophysical Union Spring Meeting, Washington, D.C., 1979.
5. H. S. Bridge *et al.*, *Eos* **60**, 305 (1979).
6. C. B. Pilcher and J. S. Morgan, *Science* **205**, 297 (1979).
7. R. E. Vogt *et al.*, *ibid.* **204**, 1003 (1979).
8. N. F. Ness, personal communication. The magnetic projection of the orbit of Io to the atmosphere of Jupiter was calculated using the GSFC O4 magnetic field model (3 February 1979 version). The location of the boundary of the magnetotail field lines in the atmosphere was provided by N. F. Ness.
9. R. M. Thorne and B. T. Tsurutani, in preparation.
10. D. M. Hunten and A. J. Dessler, *Planet. Space Sci.* **25**, 817 (1977).
11. S. K. Atreya, T. M. Donahue, B. R. Sandel, A. L. Broadfoot, G. R. Smith, *Geophys. Res. Lett.*, in press.
12. G. R. French and P. J. Gierasch, *J. Atmos. Sci.* **31**, 1707 (1974).
13. J. W. Chamberlain, *Physics of the Aurora and Airglow* (Academic Press, New York, 1961), p. 125. An IBC of III indicates that the visual brightness of the aurora is similar to that of moonlit cumulus clouds.
14. We acknowledge the untiring effort of Susan Hanson, our assistant experiment representative at the Jet Propulsion Laboratory. She was responsible for most of the detailed sequencing of our experimental observations. We also acknowledge the efforts and operations of all Voyager project personnel, who have made this mission a success. The research described in this report was carried out by the Jet Propulsion Laboratory, California Institute of Technology, under NASA contract NAS 7-100.

28 September 1979

Magnetic Field Studies at Jupiter by Voyager 2: Preliminary Results

Abstract. *Data from the Goddard Space Flight Center magnetometers on Voyager 2 have yielded on inbound trajectory observations of multiple crossings of the bow shock and magnetosphere near the Jupiter-sun line at radial distances of 99 to 66 Jupiter radii* (R_J) *and 72 to 62* R_J, *respectively. While outbound at a local hour angle of 0300, these distances increase appreciably so that at the time of writing only the magnetopause has been observed between 160 and 185* R_J. *These results and the magnetic field geometry confirm the earlier conclusion from Voyager 1 studies that Jupiter has an enormous magnetic tail, approximately 300 to 400* R_J *in diameter, trailing behind the planet with respect to the supersonic flow of the solar wind. Additional observations of the distortion of the inner magnetosphere by a concentrated plasma show a spatial merging of the equatorial magnetodisk current with the current sheet in the magnetic tail. The spacecraft passed within 62,000 kilometers of Ganymede (radius = 2,635 kilometers) and observed characteristic fluctuations interpreted tentatively as being due to disturbances arising from the interaction of the Jovian magnetosphere with Ganymede.*

The Voyager 2 magnetic field experiment, for which the instrumentation is identical to that on Voyager 1 (*1, 2*), operated flawlessly throughout the second Jupiter encounter. Here we present a brief overview of the results obtained to date on the Jovian magnetosphere, the bow shock, the magnetopause, and the extended magnetic tail. The magnetic tail was first identified during studies of Voyager 1 data (*3*). Because the radius of the tail on the dawnside of the magnetosphere is so large [150 to 200 Jupiter radii (R_J)] and the postperiapsis trajectory was at a sun-planet-spacecraft angle of 140°, Voyager 2 was immersed in the tail for approximately 2 weeks. Two crossings of the near-equatorial current sheet (plasma sheet) were observed in the magnetosphere and its tail almost every 10-hour rotation period of the planet. Hence, a definitive mapping of the geometry and character of these enhanced plasma and depressed magnetic field regions has been possible far into the nightside tail region. At periapsis the observed field is 335 nT (nanotesla), 20 percent less than the expected 425 nT; this is because of the immersion of Voyager 2 in the current sheet.

In addition, there is evidence for an interaction of the satellite Ganymede with the Jovian magnetosphere that leads to disturbances observed forward of this satellite as the Jovian magnetosphere corotates with the planet past the satellite. The character of these disturbances is complex. Their spatial location suggests that the magnetosphere may be in motion with respect to the planet at the satellite distance of 15 R_J.

In obtaining the data presented here we used averages of the basic vector field measurements (at $16^2/_3$ Hz) over intervals of 1.92 seconds, 9.6 seconds, 16 minutes, and 1 hour. As in the 30-day report on the Voyager 1 results, these data and interpretations are preliminary and based on "quick-look" data tapes and ephemerides.

Bow shock and magnetopause. Voyager 2 crossed the bow shock of Jupiter inbound at least 11 times from day 183 (2 July 1979) at 1621 universal time (UT) to

0036-8075/79/1123-0966$00.50/0

day 186, 0955 UT. This corresponds to a planetocentric distance range of 98.9 to 66.5 R_J. Figure 1 shows the trajectories of Voyager 1 and 2, as well as Voyager 1's modeled bow shock and magnetopause boundaries (*1, 2*). The first and last inbound bow shock encounters (filled circles) are shown for Voyager 2, and a representative set of Voyager 1 inbound bow shock crossings are given. Voyager 2 crossed the magnetopause three times inbound to Jupiter, the first crossing occurring on day 185 at 2337 UT and the last on day 186 at 1840 UT, also shown in Fig. 1. The upper two panels of Fig. 2 [magnetic field, B, and root mean square (rms) plotted against time] show identifications of the inbound magnetopause and bow shock crossings.

To obtain an estimate of the average bow shock normal direction over 7 of the 11 crossings, we used magnetic coplanarity where applicable and linear field component averaging for "parallel" shocks (that is, those for which the shock surface normal is parallel to the upstream magnetic field). Results in heliographic coordinates were: $\langle\lambda\rangle = 180° \pm 19°$, and $\langle\delta\rangle = 30° \pm 38°$, where λ and δ are, respectively, the longitude and latitude referenced to the solar equatorial plane ($\lambda \equiv 180°$ is sunward and $\delta \equiv 90°$ is "northward"). Because of the large variability of the data around most of the bow shock crossings, reflected in part by the large uncertainties on $\langle\lambda\rangle$ and $\langle\delta\rangle$, a meaningful comparison with the modeled hyperbolic bow shock normal ($\lambda_{model} = 160°$, $\delta \equiv 0°$) based on the Voyager 1 crossings is impossible. The second and third magnetopause crossings were analyzed by determining for each the plane of minimum variance (*4*) of the magnetic field through the transition zone using 1.92-second averages. The analyses yielded $\lambda_2 = 156°$, $\delta_2 = -3°$ for the second crossing and $\lambda_3 = 154°$, $\delta_3 = 1°$ for the third. The magnetopause crossings were classic tangential discontinuities. Analysis of the first magnetopause crossing, which was unusually broad and turbulent, has not yielded meaningful results.

As of this date (2 August 1979) no outbound shock crossings have been identified. Although no unambiguous outbound magnetopause crossings have been distinguished, the magnetic field data on days 204 to 206 show characteristics of the magnetosheath. However, periods in which the data were similar to those obtained when the spacecraft was in the tail were also observed during these and many following days. As shown in Fig. 2, an obvious change in the character of the field, on this time scale, had taken place during days 204 to 206. Before this period, starting at about the beginning of day 193 (35 R_J) the field appeared in all respects like a magnetospheric tail; this region will be discussed below. The data gap from day 204, 1616 UT to day 205, 0036 UT is due to permanent data loss during a spacecraft trajectory course maneuver.

Since no clear Voyager 2 outbound magnetopause crossing has yet been identified, it is impossible to derive an accurate estimate of an average modeled magnetopause surface. However, since the magnetopause as observed by Voyager 1 was successfully modeled by an x-axis symmetric parabola in Jupiter's orbital plane, a similar geometry was used to predict the region where Voyager 2 outbound might be expected to encounter the magnetopause. This curve depends only on the average position of the Voyager 2 inbound magnetopause crossings and the average normal to that surface at that point. From the results of analyzing multiple intervals associated with the second and third crossings, this normal is $\langle\lambda\rangle = 152°$, $\langle\delta\rangle = 0°$. This information is sufficient to produce the modeled Voyager 2 magnetopause (MP-V2) shown in Fig. 1, which is analytically represented by $y = \pm\ 10.1(68.2 - x)^{1/2}$, where x and y are in units of R_J. This curve intersects the outbound trajectory on midday 208, and yields a solar wind stagnation point of 68 R_J. The uncertainty in the estimated average inbound bow shock normal is obviously too large for us to use a similar procedure for the bow shock.

Magnetosphere structure. From Fig. 2, it is clear that a principal feature of the magnetic field observations throughout the encounter is the persistent 10-hour periodicity in the occurrence of two dips in the field magnitude each accompanied by an increase in the Pythagorean mean rms. These events correspond to traversals of the near-equatorial current sheet of the inner magnetosphere or to traversals or close approaches to the plasma sheet in the magnetic tail. They are quite similar to the events shown in figure 4 of the Voyager 1 report (*2*).

Inbound and near Jupiter the magnetic field vector is always directed southward, consistent with the polarity of the main planetary field. In the tail, beyond 50 R_J, the vector tends to be parallel to the plasma sheet and the expected position of the magnetopause. The field depressions are often very significant, amounting to 80 percent or more of the ambient field on either side of the event. Multiple traversals or close approaches to the current or plasma sheet are also often seen. Away from the current (plasma) sheet, the field tends to slowly increase to a maximum at a point nearly midway between the adjacent sheet crossings, and the rms is very small. The

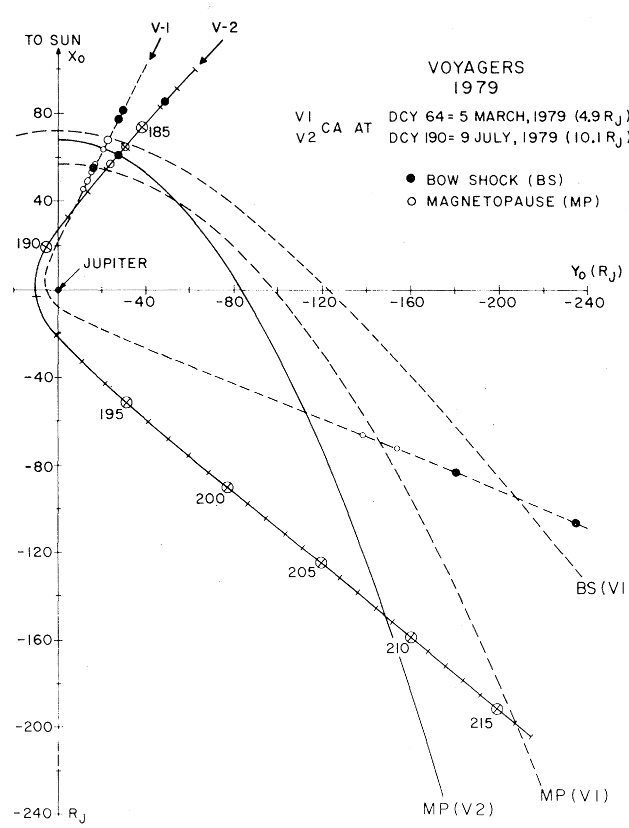

Fig. 1. Voyager 1 (dashed lines) and Voyager 2 (solid lines) Jupiter encounter trajectories in planetocentric orbital coordinates (x-y plane is the orbital plane, $+x$ toward the sun, and $+z$ northward). The day of the year is labeled on the trajectories. Voyager 2 remained within 15 R_J of Jupiter's orbital plane over the interval shown. The modeled bow shock (hyperbola) and magnetopause (parabola) curves are based on average Voyager 1 and 2 crossings. (*CA*, closest approach.)

direction of the field is nearly radial with respect to Jupiter close to the planet and outbound beyond 50 R_J where the characteristic tail geometry becomes dominant.

As the spacecraft left Jupiter, the character of the field changed from roughly dipolar with superimposed depressions near the sheet crossings to a tail configuration. Figure 3 shows the 8-day interval from periapsis to 108 R_J, illustrating the orientation of the field vector. The nearly step function nature of the two angles λ, δ testifies to the clear distinction of the field line source, that is, northern ($\lambda \sim 0°$ to $20°$) or southern ($\lambda \sim 180°$ to $200°$) hemisphere. Close to Jupiter ($R < 30$ R_J), δ is always significantly negative (that is, southbound) but beyond that point δ approaches zero as the tail field configuration is developed.

There are a few specific and, we believe, significant exceptions to the general observations described above. Just after crossing the magnetopause while inbound, and continuing for approximately 30 hours thereafter, the magnetic field magnitude and direction fluctuated considerably. The field remained generally southward directed but there was no evidence of a 10-hour periodicity in either magnitude or direction. The general appearance of the data and the magnitude of the field distinguishes the region clearly from the magnetosheath; it appears to be a type of boundary layer between the sheath and the corotating magnetosphere. Further examination of this particular period of data will benefit by comparisons with data from other instruments on Voyager 2 and also with data from Voyager 1 and Pioneer 10 and 11.

The periapsis distance of Voyager 2 was 10.1 R_J, twice that of Voyager 1 (4.9 R_J) and much more than those of Pioneer 10 and 11 (2.8 and 1.7 R_J). As a result, it has not been possible to conduct an analysis of the main planetary field in the same manner used in these earlier studies, since the observations contain important and nonuniform contributions from localized sources near the spacecraft. Figure 4 illustrates this point, where a comparison of the expected planetary field (*5*) is made with the observed field magnitude. The large depressions that occur near the equator crossings almost merge into a continuously depressed field while the spacecraft is within 16 R_J of the surface of Jupiter. We have chosen to postpone any quantitative analysis of the main field, because of the large contribution from local and external sources. Data from Voyager 1 (*1, 2*) showed that the dipole term was smaller by 5 percent than that obtained by Pioneer 11. This was interpreted as being due to the magnetic field of the current sheet; even though the maximum field for Voyager 1 was eight times that of Voyager 2, the contributions from external sources were important. As Fig. 4 shows, the perturbations in magnitude amount to as much as 30 percent of the background field, so that the energy density of the field itself has been reduced by one-half.

Tail structure and dynamics. As with Voyager 1, the current sheet in the near-planet tail was found to be a broad feature with relatively shallow depressions in field magnitude. In these respects it more closely resembles the dayside current sheet than that of the more distant tail. There the sheet crossing signature in the magnetic field is generally a very rapid direction change together with a deep depression in the field magnitude to near zero. In Fig. 5 the spacecraft locations at the times of magnetotail sheet crossings are shown. Figure 5a also includes curves giving the sheet crossing longitudes as functions of radial distance according to various theoretical models: the rigid magnetodisk (*6*) and two nonrigid models (*7, 8*).

The observed crossings agree with the rigid model near the planet, as previously observed (*1, 2*), and then gradually exhibit an increasing delay with increasing radial distance. An asymmetry is found between the two types of crossings, however. The north-to-south crossings tend to follow the curve for the model of Kivelson *et al.* (*7*), but the return crossings do not. The south-to-north sheet crossings most nearly agree with the model of Northrop *et al.* (*8*), but that model does not fit the north-to-south

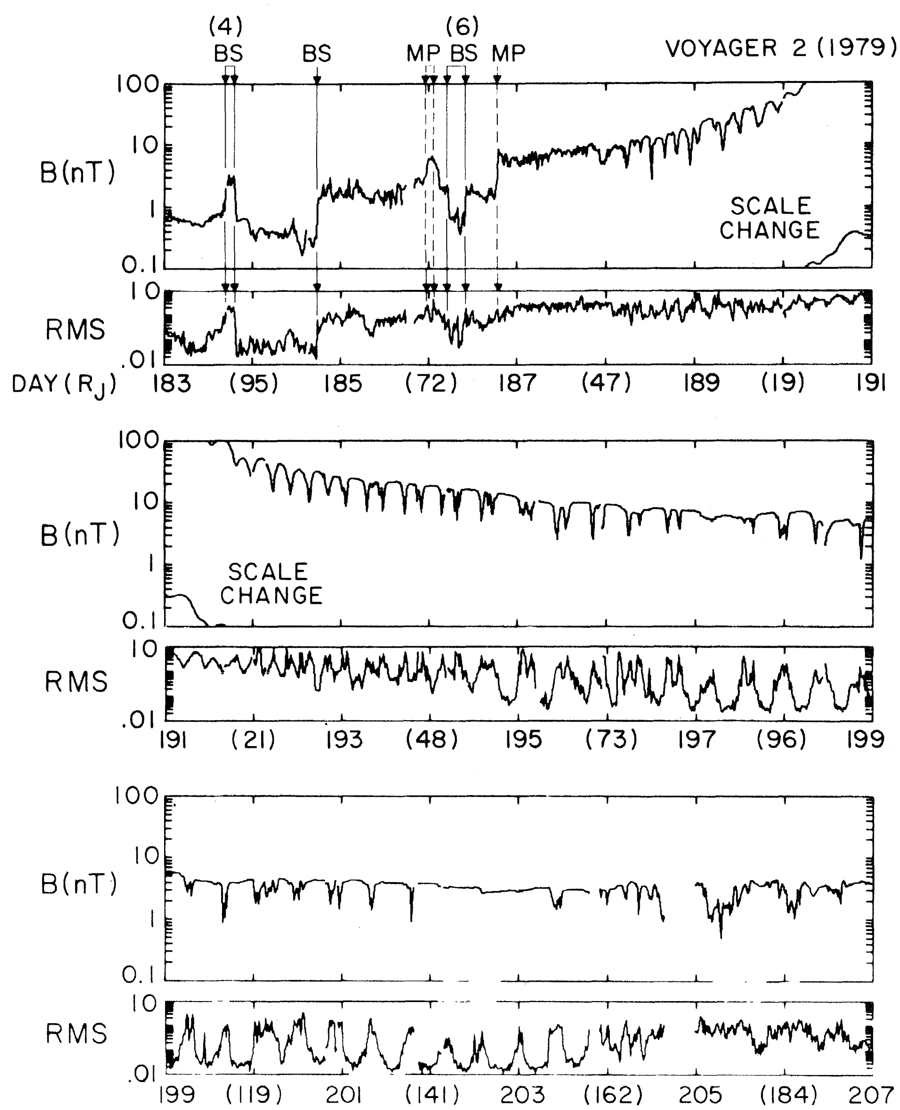

Fig. 2. Magnetic field magnitude (*B*) and Pythagorean mean rms deviation (16-minute averaging intervals) for − 8/+ 16 days around closest approach to Jupiter which occurred at 2230 UT on day 190, 9 July 1979. Inbound bow shock (*BS*) and magnetopause (*MP*) crossing times are denoted, as are plot scale changes. R_J refers to Voyager 2's planetocentric distance at the beginning of each even-numbered day.

crossings. A lack of symmetry was also observed by Voyager 1, where the south-to-north longitudes were not too different from those expected for the rigid model, whereas the north-to-south crossings were closer to the curve for a disk with spiral distortion.

In Fig. 5b the current sheet crossings are shown in terms of the solar magnetospheric coordinate z_{SM}. The solar magnetospheric (SM) coordinates form a right-handed, nonrotating, orthogonal system defined such that x_{SM} is directed from the planet to the sun and z_{SM} lies in the plane containing the x_{SM} axis and **M**, the magnetic dipole moment of the planetary field. Voyager 1 showed that within a radial distance of 25 R_J, the current sheet crossings occurred nearly coincident with the spacecraft traversal of the magnetic equatorial plane, while in the outer portion of the outbound traversal of the predawn magnetosphere, the sheet crossings occurred generally near or south of the SM equatorial plane (*3*). Voyager 2 data support this view in which at increasing planetocentric distances there is a transition from an equatorial current sheet to a tail current sheet which is approximately parallel to the SM *xy*-plane, although somewhat south of it, as shown in Fig. 5b. Figure 5, a and b, illustrates the temporal variability of the Jovian magnetotail structure. On four occasions at $R < 140\ R_J$ complete crossings of the current sheet were not observed, although perturbations of the magnetic field were seen.

Figure 6 shows hourly average tail field vector components projected on the SM equatorial plane. The length of the field vectors was scaled logarithmically as $K\ (1 + \log B_{xy})$, with representative values of 1 and 100 nT illustrated. The periodic traversal of the current sheet behind the dawn-dusk meridian to a distance of $\sim 96\ R_J$ is evident in the alternating direction of the vectors in this projection. There may also have been additional traversals at greater distances. Other than the data near the end of the trajectory segment shown, the few vectors in Fig. 6 that do not have the characteristic magnetotail orientation represent hours dominated by current sheet crossings, with changing azimuthal direction and a large, generally southward z component. North (south) of the current sheet the field was directed parallel (antiparallel) to $\lambda \sim 18°$ in the near-planet portion of the tail, veering gradually to $\lambda \sim 12°$ or less at greater distances.

Thus Voyager 2 has confirmed that current sheet crossings in the more distant ($x_{SM} < -25\ R_J$) magnetotail are not symmetrical with respect to occurrence longitude in contrast to predictions by the various existing theories. The crossings are reasonably well understood in terms of a periodic rocking of the tail current sheet about the longitudinal axis of the tail, as Jupiter rotates, in a fashion similar to that observed in Earth's magnetotail. Temporal variations are sometimes seen which perturb the normally steady magnitude and direction of the tail field and alter the location as well as other characteristics of the current sheet for periods of hours. Whether these disturbances are due to external (solar wind) variations or to internal dynamical processes is not yet known but may be clarified through careful correlation of simultaneous observations (with appropriate time delay) by Voyager 1 and 2.

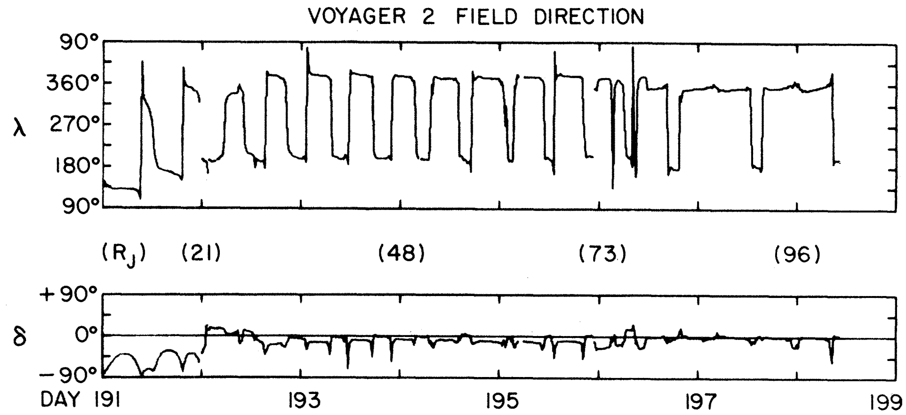

Fig. 3. The direction of the magnetic field in heilographic coordinates, λ (longitude) and δ (latitude) (16-minute average intervals) for the period day 191 to midday 198; see text for definition of coordinates. Measurements made during the few times that the spacecraft was rolling have not been deleted.

Disturbances near Ganymede. Voyager 2 flew by Ganymede at a distance of 62,000 km from the satellite center, as shown in Fig. 7. We will consider the interaction between Ganymede and the Jovian magnetosphere to be expected on the basis of magnetohydrodynamic (MHD) theory, assuming that Ganymede, like our moon, has no magnetic field, no atmosphere, and very low electrical conductivity of its upper layers. On the basis of an electron density of 1.5 cm^{-3}, the theoretical corotational speed of 177 km/sec, a magnetic field magnitude of 120 nT, and a heavy ion mix typical of Voyager 1 torus observations, we obtain an Alfven Mach number of $M_A = 0.26$, that is, $M_A^2 \ll 1$. Breakdown of corotation (*9*) and an appreciable contribution of protons would strengthen this conclusion. Assuming further that $M_s^2 \gg M_A^2$, where M_s is the sonic Mach number, we expect that there will be no bow shock, since $M_A < 1$.

Flux-tubes moving with their initial flow speed will be emptied of some of their plasma while passing Ganymede, but they will not be deflected appreciably. The void will generate a rarefaction wave with plasma filling in from above and below. As the flux-tube moves, rarefaction wave fronts propagate in both directions along **B** at the speed of sound. The rarefaction region will not extend perpendicular to **B**, because of the dominance of magnetic field pressure. Thus it has the shape of a "delta-wing" of thickness 2 R_G (where R_G is the radius of Ganymede) and an opening angle of $2\theta_s = 2 \tan^{-1} (M_s^{-1})$. The resulting pressure imbalance will cause a slight inward bending of field lines towards the rarefaction region leading to a small, broad depression in B outside the wing and a small increase in B inside. The bending produces Alfven waves in a delta-wing shaped region with an opening angle $2\theta_A = 2 \tan^{-1} (M_A^{-1})$, which is larger than $2\theta_s$. We expect the Alfvenic perturbations to be concentrated toward the front edge of the wing. Deviations from this simple MHD picture are expected because of finite gyro-radius effects (especially at the boundary of the rarefaction region), and nonstationary processes. Last but not least, an internal magnetic field (*10*), a tenuous atmosphere consistent with data from the Voyager 1 ultraviolet spectrometers (*11*), or higher electrical conductivities would change this picture.

Let us now consider the magnetic field observations made near Ganymede. Unusual fluctuations in the 9.6-second averages of the magnitude of **B** and large rms variations over 9.6-second average intervals were observed between $\sim$ 0350 and 1200 UT on day 190 (9 July 1979). The position of the spacecraft during this interval is indicated by the dashed lines in Fig. 7. The disturbed region extended from approximately 61 to $-56\ R_G$ along y, 12.5 to 39 R_G along x, and -9 to -27 R_G along z. The nature of the disturbances in the magnetic field intensity is

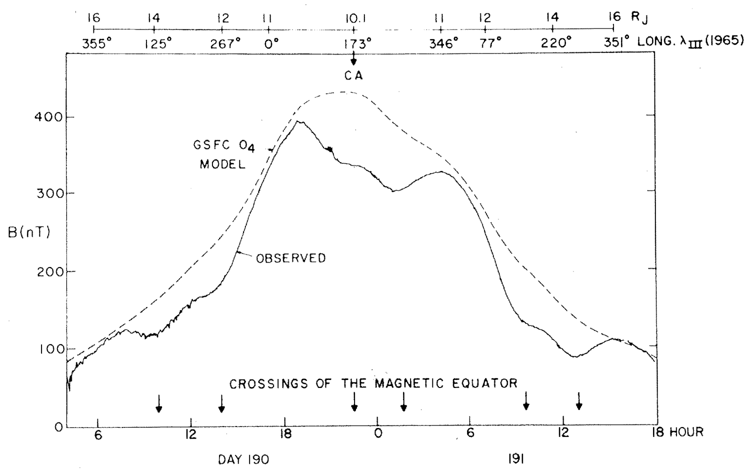

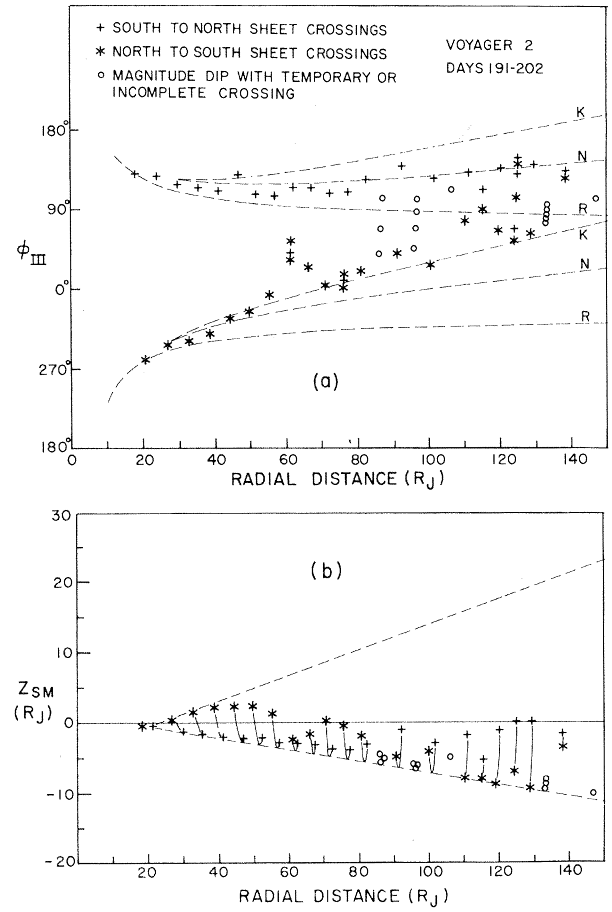

Fig. 4 (above). Comparison of magnitude of the observed magnetic field (48-second averaging intervals) with that of GSFC O_4 Jupiter planetary magnetic field model (*5*) for 38 hours around closest approach to Jupiter. Fig. 5 (right). (a) Location in Jovicentric distance and system III longitude of current sheet crossings and perturbed field regions in the magnetotail out to a radial distance of 150 R_J. Dashed curves indicate crossing longitudes as functions of radial distance predicted by the rigid rotating disk model (*R*) as well as the models of Kivelson *et al.* (*K*) and Northrop *et al.* (*N*). (b) Location of sheet crossings in terms of the solar magnetospheric (*SM*) *z*-coordinate (see text) of Voyager 2 during the magnetotail passage. In cases of multiple traversals, as shown in (a), only the final complete traversal of the series is shown for clarity. Those segments of the z_{SM} versus *R* position curve that indicate location south of the current sheet are shown, while the dashed lines indicate the full extent of the oscillations of the spacecraft location in this coordinate system.

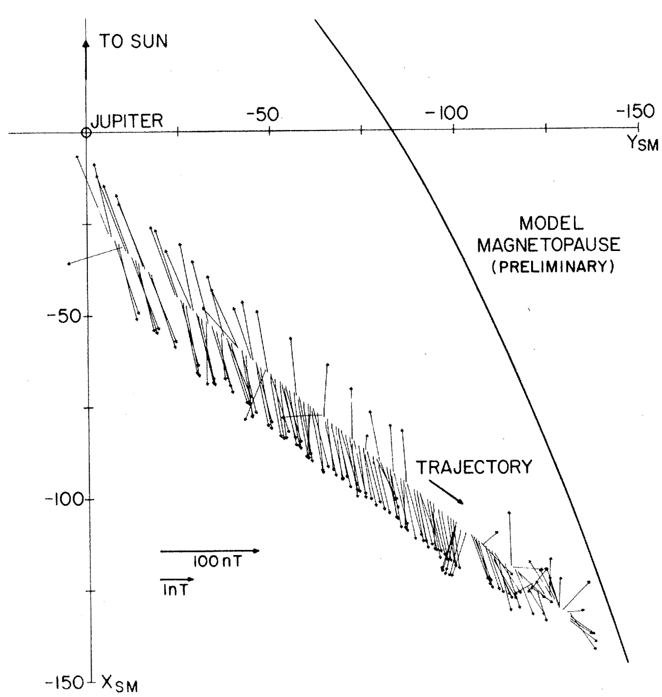

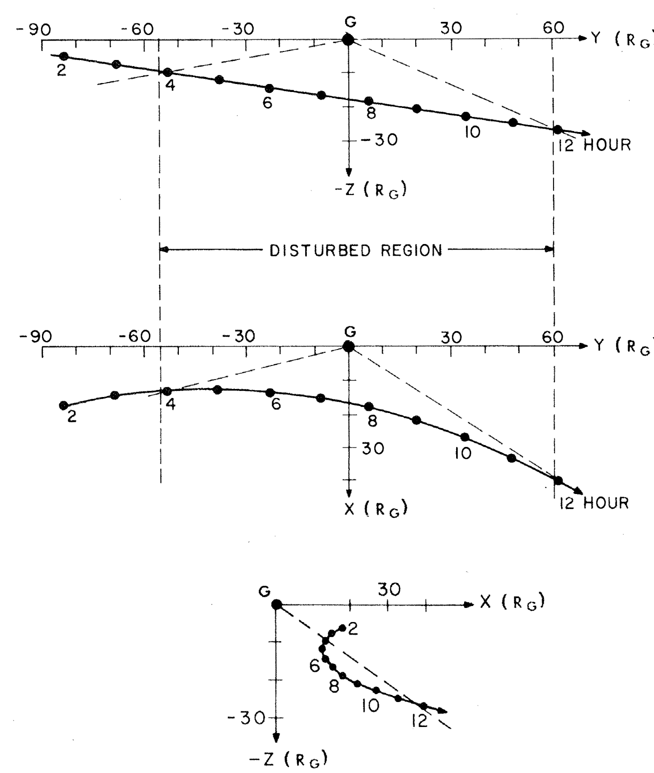

Fig. 6 (left). Projection of hourly average magnetic field components on the solar magnetospheric *xy*-plane along the Voyager 2 outbound trajectory. Only the field vectors corresponding to even hours have been plotted. The transition from a generally steady and uniform orientation throughout the tail to the intermittent observation of disoriented magnetosheath field near the end of the data shown is clearly seen. Fig. 7 (right). Trajectory of Voyager 2 in the neighborhood of Ganymede (*G*), showing the location of the region in which the magnetic field was disturbed. The *y*-axis points toward Jupiter, the *x*-axis points in the corotation direction, and the *z*-axis forms a right-handed satellite centered coordinate system. Distances are measured in units of Ganymede radii (R_G = 2635 km).

illustrated in Fig. 8. The following characteristics of the disturbances are particularly significant: (i) the size of a perturbation, ΔB, is $\lesssim$ 5 nT in a background field of 60 to 160 nT; (ii) the duration is typically of the order of a minute; (iii) an exceptionally large negative perturbation ($\Delta B < 0$) is usually preceded or followed by a large positive perturbation; (iv) large positive and negative perturbations may occur in nearly symmetrical pairs (Fig. 8, a and b) in which the negative perturbations are on the outside and the positive perturbations are on the inside. Another characteristic of the disturbances in B, not illustrated in Fig. 8, is that the perturbations $\mathbf{\Delta B} = \mathbf{B} - \langle \mathbf{B} \rangle$ are primarily along $\langle \mathbf{B} \rangle$. These small longitudinal perturbations are unlike the large transverse field perturbations observed near Ganymede's L-shell at rather large distances from Ganymede by Pioneer 11 (*12*).

Comparing the magnetic field observations with the plasma fluxes observed by the plasma spectrometer (*13*) we found that most of the large perturbations in B occur at a boundary where the plasma flux changes abruptly. The negative perturbation is always on the higher flux side of the boundary. When pairs of perturbations are observed, as in Fig. 8, a and b, there is a lower flux region between them. The magnitude and sign of the perturbations in B are similar to those which one expects to observe as a result of magnetization and perpendicular gradient drifts at the edge of a low-β cavity. We cannot, however, exclude the possibility that the field perturbations might also be due to other causes such as waves generated by instabilities in a sheath.

There are at least three conceivable sources of the perturbations discussed above: Ganymede and its wake; the Jovian current sheet; and a temporal magnetospheric disturbance (for example, a substorm). The possibility that Ganymede is the source of the perturbations is suggested by their proximity to it and by the fact that they are observed at nearly equal distances toward and away from Jupiter relative to Ganymede. They are not associated with just the orbit of Ganymede, since the fluctuations were not observed by Voyager 2 when it passed near the orbit as it was outbound from Jupiter on day 191. The Jovian current sheet was observed by Voyager 2 at about 0330, 1000, and 1315 UT on day 190 (9 July). Fluctuations observed during hour 10 might be related to the current sheet, but most of the fluctuations discussed above were observed away

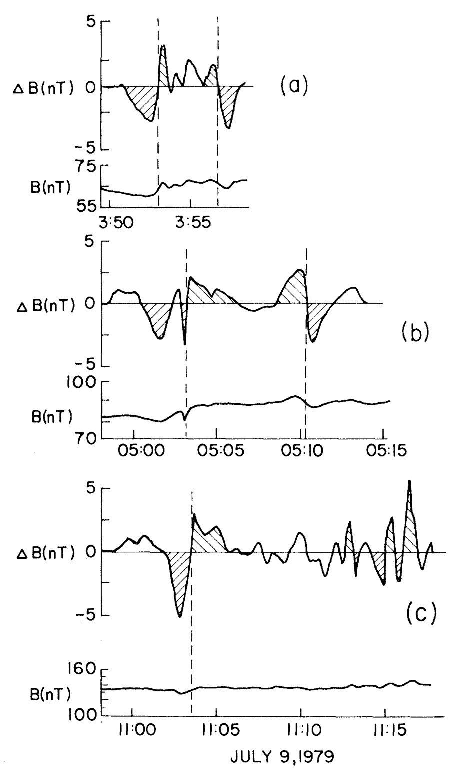

Fig. 8. Examples of perturbations in the 9.6-second averages of the magnetic field intensity, B, observed near Ganymede. ΔB is the change in intensity measured with respect to a 4-minute running average of B.

from the center of the current sheet. Conversely, no disturbances were seen near the current sheet at about 1315 UT. These results suggest that the current sheet was not the primary cause of the fluctuations observed near Ganymede. The possibility that the disturbances are due to a transient magnetospheric event cannot be excluded. However, it implies that the event began just as the spacecraft was at $y = -56\ R_G$ and ended when the spacecraft was at $y = 61\ R_G$, which seems unlikely. Furthermore, substorm-related perturbations in **B** are likely to be transverse to **B** because of field-aligned currents (*12*), whereas we have observed perturbations that are nearly along **B**.

If the disturbances are to be attributed to Ganymede, then one must explain how they are generated and why they are seen at relatively large distances from Ganymede. Since the magnetic perturbations have the form that one expects to be associated with a current in a sheath surrounding a cavity, they can be produced by creating low-density regions, which is what happens when the magnetosphere rotates past Ganymede as explained above. The observation of perturbations associated with low flux regions as far as $y = \pm 60\ R_G$ can be explained by strong deviations from corotational plasma flow, both in magnitude and direction. We may, for example, postulate long-wavelength Alfven waves propagating along Jupiter's magnetic field with an amplitude of $\pm 2\ R_J$. In order to explain the tens of large disturbances that were observed in an 8-hour period, one requires Alfven waves with periods of the order of 30 minutes. For an Alfven speed of the order of 1000 km/sec, this implies wavelengths of the order of 25 R_J. Such waves may be due to resonant oscillations in the Jovian magnetosphere at the position of Ganymede, analogous to those that are assumed to be related to pulse-continuous oscillations at Earth. The existence of Alfven waves implies the existence of small fluctuations in the direction of **B** with a period of the order of 30 minutes. The waves would have a radial component of velocity directed alternately inward and outward with a speed of the order of $|\delta B|\ V_A/B_0 \approx 100$ km/sec. Finally, the motions produced by such waves would also tend to produce a relatively broad region in which energetic particles are swept out by Ganymede. Thus, the hypothesis that Alfven waves might be present and cause a disturbance produced by Ganymede to extend to $y = \pm 60\ R_G$ can be tested in future studies with the particle and field data. An alternative source of bulk plasma motions may be provided by interchange instabilities associated with the outward transport of plasma.

NORMAN F. NESS
MARIO H. ACUNA
RONALD P. LEPPING
LEONARD F. BURLAGA
KENNETH W. BEHANNON
Goddard Space Flight Center, Greenbelt, Maryland 20771
FRITZ M. NEUBAUER
Technische Universitat, Braunschweig, Federal Republic of Germany

References and Notes

1. K. W. Behannon, M. H. Acuna, L. F. Burlaga, R. P. Lepping, N. F. Ness, F. M. Neubauer, *Space Sci. Rev.* **21**, 235 (1977).
2. N. F. Ness, M. H. Acuna, R. P. Lepping, L. F. Burlaga, K. W. Behannon, F. M. Neubauer, *Science* **204**, 982 (1979).
3. N. F. Ness, M. H. Acuna, R. P. Lepping, K. W. Behannon, L. F. Burlaga, F. M. Neubauer, *Nature (London)*, in press.
4. B. U. O. Sonnerup and L. J. Cahill, *J. Geophys. Res.* **72**, 171 (1967); G. L. Siscoe, L. David, Jr., P. J. Coleman, Jr., E. J. Smith, D. C. Jones, *ibid.* **73**, 61 (1968).
5. M. H. Acuna and N. F. Ness, *ibid.* **81**, 2917 (1976).
6. J. A. Van Allen, B. A. Randall, D. N. Baker, C. K. Goertz, D. D. Sentman, M. F. Thomsen, H. R. Flindt, *Science* **188**, 459 (19 C. K. Goertz, *J. Geophys. Res.* **81**, 3368 (1976); also see review by C. K. Goertz, *Space Sci. Res.* **23**, 319 (1979).
7. M. G. Kivelson, P. J. Coleman, L. Froidevaux, R. L. Rosenberg, *J. Geophys. Res.* **83**, 4823 (1978).

T. G. Northrop, C. K. Goertz, M. R. Thomsen, *ibid.* **79**, 3579 (1974).
9. R. L. McNutt, Jr., J. W. Belcher, J. D. Sullivan, F. Bagenal, H. S. Bridge, *Nature (London)* **280**, 803 (1979).
10. F. M. Neubauer, *Geophys. Res. Lett.* **5**, 905 (1978).
11. A. L. Broadfood *et al.*, *Science* **204**, 979 (1979).
12. M. G. Kivelson and G. R. Winge, *J. Geophys. Res.* **81**, 5853 (1976).
13. J. Belcher and H. S. Bridge, personal communication.
14. We thank our colleagues in the Voyager Project for discussions of these early results and the entire Voyager team for the success of this experiment. We also thank G. Sisk, E. Franzgrote, M. De Gyurky, and C. Brower of JPL for their support; C. Moyer, J. Scheifele, J. Seek, and E. Worley for contributions to the design, development, and testing at GSFC of the experiment instrumentation; and G. Burgess, T. Carleton, C. Cressy, P. Harrison, D. Howell, W. Mish, L. Klein, L. Moriarty, A. Silver, M. Silverstein, K. Simms, and T. Volmer of the data analysis team at GSFC. Finally, we thank J. W. Belcher and H. S. Bridge for allowing us to refer to their plasma data in regard to the Ganymede-related perturbations. The possibility that these disturbances might extend over a relatively large distance from Ganymede was noted by one of us in a discussion with J. Belcher concerning a plot of plasma data which he prepared. One of us, F.M.N., was supported financially by the German Ministry of Science and Technology.

26 September 1979

Plasma Observations Near Jupiter: Initial Results from Voyager 2

Abstract. *The first of at least nine bow shock crossings observed on the inbound pass of Voyager 2 occurred at 98.8 Jupiter radii* (R_J) *with final entry into the magnetosphere at 62* R_J. *On both the inbound and outbound passes the plasma showed a tendency to move in the direction of corotation, as was observed on the inbound pass of Voyager 1. Positive ion densities and electron intensities observed by Voyager 2 are comparable within a factor of 2 to those seen by Voyager 1 at the same radial distance from Jupiter; the composition of the magnetospheric plasma is again dominated by heavy ions with a ratio of mass density relative to hydrogen of about 100/1. A series of dropouts of plasma intensity near Ganymede may be related to a complex interaction between Ganymede and the magnetospheric plasma. From the planetary spin modulation of the intensity of plasma electrons it is inferred that the plasma sheet is centered at the dipole magnetic equator out to a distance of 40 to 50* R_J *and deviates from it toward the rotational equator at larger distances. The longitudinal excursion of the plasma sheet lags behind the rotating dipole by a phase angle that increases with increasing radial distance.*

This is a preliminary report of results obtained by the Voyager plasma experiment during the encounter of Voyager 2 with Jupiter from about 100 R_J before periapsis to about 300 R_J after periapsis. The instrument is identical to that flown on Voyager 1 (*1*) and has been described in detail in (*2*). We discuss here (i) the crossings of the bow shock and magnetopause observed on the inbound and outbound passes, (ii) the radial variation of plasma properties in the magnetosphere, (iii) variations in plasma properties near Ganymede, (iv) corotation and composition of the plasma in the dayside magnetosphere, and (v) plasma sheet crossings observed on the inbound and outbound passes.

It is interesting to compare the Voyager 2 results with those of Voyager 1, and in this regard some differences between the trajectories of the two spacecraft should be borne in mind as well as some limitations of the preliminary analysis used for both data sets. Figure 1 shows the trajectories of the two spacecraft projected onto the equatorial plane of Jupiter. The closest approach to Jupiter was 4.9 R_J for Voyager 1 and 10.1 R_J for Voyager 2. A second significant difference is the angle between the asymptote to the outbound trajectory and the Jupiter-sun line, ~ 115° for Voyager 1 and ~ 133° for Voyager 2. As a consequence of these differences in the trajectory, Voyager 2 did not penetrate the dense plasma of the Io torus and data were obtained only in the region referred to in (*1*) as the outer magnetosphere. It is apparent from Fig. 1 that the trajectory of Voyager 2 was better suited to study a possible Jovian magnetotail than that of Voyager 1 and this fact is evident in some observations discussed below.

A detailed analysis of the positive ion and electron data obtained during the Voyager encounters with Jupiter is in progress, but definitive results for plasma parameters will not be available for some time. We have used a crude first-order analysis that gives a lower limit for the number density of positive ions and a good estimate of the variation of the electron intensity with distance. The ion densities in this report and in (*1*) should be taken as lower limits since two important effects have been neglected in the preliminary analysis: first, the geometrical response which depends on the Mach number and direction of the flow has been treated in a very approximate way and, second, calculation of the number density, n, depends on the composition of the ions. We have computed n assuming that the positive ions are protons, but most of the low-energy ions have $A/Z^* > 8$ (*3*) (A is atomic mass number and Z^* is effective charge number); hence the actual density has been underestimated by about a factor of 3. The positive ion number densities and electron intensities computed in this way for Voyager 1 and 2 are believed to be directly comparable, and relative values at the same radial distance are probably accurate to better than a factor of 2.

Table 1 includes all boundary crossings separated by an interval greater than 96 seconds that occurred on the inbound pass, and is complete for the outbound pass to 1703 UT on day 215. Many of the observed bow shock crossings, as well as all the bow shock crossings observed by Voyager 1, were of the laminar type. However, the first bow shock crossing observed by Voyager 2 was of the pulsation type (*4*); as expected for a pulsation shock, wave disturbances were observed upstream of the shock. These upstream waves had periods of the order of 5 minutes and were evident in the plasma density and other parameters.

The number of boundary crossings was large, and it was not possible to show individual events along the trajectory plot of Fig. 1. Thus the locations of the first and last bow shock crossings observed along the inbound trajectory of Voyager 2 are shown on the appropriate trace in Fig. 1, and the first and last magnetopause crossings are shown in a similar way. For comparison, similar first and last locations of the boundaries seen during the Voyager 1 encounter are indicated on the Voyager 1 trajectory. Data for magnetopause and shock crossings observed on the outbound trajectory of Voyager 2 are not yet complete; the first magnetopause and shock crossings are shown but there may be additional crossings after day 215. Although there are boundary layer effects, normal magnetosheath plasma is observed on the outbound pass; for example on day 206 at 1030 UT the shocked solar wind in the magnetosheath had an ion number density of 0.7 cm^{-3}, a flow speed of 325 km/sec from 15° east of the spacecraft-sun line, a thermal speed of ~ 100 km/sec, and a momentum flux density of ~ 770 eV/cm^3. Most of the ions in the magnetosheath are protons.

All the magnetopause crossings, with the exception of two during the outbound pass, occurred at subspacecraft system III (1965.0) longitudes ranging from 225° to 33°, with 9 out of 14 crossings in the range 225° to 351°, in fair

 0036-8075/79/1123-0972$01.25/0